Research Square

Preprints are preliminary reports that have not undergone peer review.
They should not be considered conclusive, used to inform clinical practice,
or referenced by the media as validated information.

Patient-derived organoids inform treatment response and clinical outcomes in tumors of uncertain differentiation

Qian Kong
Shanghai Sixth People's Hospital
Lina Tang
Shanghai Sixth People's Hospital
Chenming Zhong
Tongren Hospital
Yujing Huang
Shanghai Sixth People's Hospital
Chenghao Yin
Shanghai Sixth People's Hospital
Yunyu Wang
Shanghai Sixth People's Hospital
Hao Luo
Shanghai Sixth People's Hospital
Qingcheng Yang
Shanghai Sixth People's Hospital
Dongdong Cheng
Shanghai Sixth People's Hospital
Yonggang Wang
Shanghai Sixth People's Hospital
Dongxi Xiang
Renji Hospital
Aina He
ainahe@sjtu.edu.cn

Shanghai Sixth People's Hospital

Article

Keywords: Patient-derived organoids, Precision oncology, Tumors of uncertain differentiation, Drug sensitivity profiling, Soft tissue sarcoma

Posted Date: October 11th, 2026

DOI: https://doi.org/10.21203/rs.3.rs-11003195/v1

License: This work is licensed under a Creative Commons Attribution 4.0 International License. Read Full License

Additional Declarations: No competing interests reported.

Abstract

Tumors of uncertain differentiation (TUD) are rare and heterogeneous with poor prognosis. In this study, We investigated the potential clinical utility of patient-derived organoid (PDO) in precision treatment of TUD. Patients whose subsequent treatment decisions guided by PDO drug sensitivity results comprised the PDO-guided cohort, while a contemporaneous cohort treated without PDO guidance served as the control cohort. 12 of 13 (92.3%) PDO-guided patients showed concordant clinical outcomes. PDO-guided cohort had superior median cumulative PFS (18.88 vs. 6.22 months, P = 0.016) and first-line PFS (2.00 vs. 1.77 months, P = 0.046) versus controls. In intra-patient analyses, 4 of 7 evaluable patients achieved an Effective PFS ratio ≥ 1.3, and all evaluable PDO-guided patients had PFS1/DFS ratios > 1.3, whereas ratios were generally < 1.3 in the control cohort. Marked inter-patient heterogeneity in drug responses was observed in PDO drug sensitivity profiling. Doxorubicin plus immune checkpoint inhibitors (ICI) showed higher inhibitory activity. Patients with more prior lines of therapy showed lower maximal PDO inhibition (r = -0.46, P = 0.024). Furthermore, patients with higher PDO inhibitory activity experienced a significantly longer time to the appearance of new lesions (24.00 vs. 8.00, log-rank P = 0.044). These findings support the clinical relevance of PDO-based drug sensitivity profiling for individualized treatment in TUD. PDO profiling may provide a complementary approach to precision treatment in this rare and highly heterogeneous group of malignancies.

Background

Tumors of uncertain differentiation (TUD) comprise a heterogeneous group of soft tissue neoplasms with an uncertain or poorly defined line of differentiation. In this study, the TUD cohort included synovial sarcoma, epithelioid sarcoma, clear cell sarcoma, alveolar soft part sarcoma (ASPS), spindle cell sarcoma and undifferentiated sarcoma. According to the World Health Organization (WHO) classification of soft tissue and bone tumors, these sarcomas are characterized by complex morphological features and the absence of identifiable lineage-specific differentiation[1]. The rarity, pathological complexity and scarcity of targetable molecular drivers make therapeutic decision-making challenging[2,3]. Treatment option is largely guided by histological subtype, disease stage, prior treatment exposure and clinical judgement, while responses to systemic therapies remain modest and vary considerably between patients[4,5].

Precision oncology has expanded treatment selection through genomic profiling and biomarker-guided strategies. However, molecular information alone may not reliably predict therapeutic response, particularly in rare and heterogeneous malignancies, as only a proportion of patients receiving genotype-matched therapies achieve meaningful clinical benefit[6]. Functional approaches that directly assess tumor responses to therapeutic agents may therefore complement genomic profiling by providing patient-specific information on drug sensitivity[7,8].

Patient-derived organoids (PDOs) have emerged as promising tools for precision oncology, enabling ex vivo assessment of tumor-specific therapeutic responses while preserving key histological and genomic characteristics of their parental tumors[9,10]. Clinical studies have demonstrated concordance between PDO drug responses and subsequent treatment outcomes in metastatic gastrointestinal cancers[11] and PDO-based approaches have also been explored in breast, gynecological, and other solid tumors[12–14].

However, PDOs remain insufficiently investigated in rare mesenchymal malignancies such as sarcomas, as previous studies have largely focused on epithelial cancers[9,11]. In TUD, PDO-based drug sensitivity profiling may provide complementary functional information for treatment selection, but evidence linking PDO-guided treatment to clinical outcomes remains scarce. We therefore established a PDO-based drug sensitivity profiling platform for TUD and evaluated its biological fidelity, drug response heterogeneity, and potential clinical relevance for individualized treatment[11].

Results

a Establishment of the PDO-guided cohort. **b** Schematic workflow of PDO establishment and drug sensitivity assessment. **c** Baseline characteristics of patients included in the PDO-guided cohort. The heatmap summarizes clinicopathological features. **d** Establishment of the control cohort. **e** Kaplan-Meier analysis of cumulative progression-free survival (PFS) duration between the PDO-guided and control cohorts. The analysis included patients with evaluable progression-free survival intervals. DSA, drug sensitivity analysis.

Establishment of PDO and control cohorts for clinical outcome analysis in TUD.

We first established a PDO patient cohort by enrolling patients with TUD. Tumor specimens were subsequently collected from these patients for PDO generation and ex vivo drug sensitivity assessment (DSA)(Fig. 1a, b).

A total of 27 tumor specimens were collected for PDO generation, and 24 patients underwent PDO-DSA.Three samples were excluded because DSA could not be completed due to insufficient live cell numbers. Among the 24 patients, 13 patients received subsequent PDO-guided treatment decisions with clinical follow-up and were included in the PDO-guided cohort for clinical outcome assessment. (Fig. 1a). The median age was 44 years (range, 13–70 years), and 9 patients (69.2%) were male. Histological subtypes included undifferentiated pleomorphic sarcoma (UPS; n = 5),

synovial sarcoma (n = 3), epithelioid sarcoma (n = 2), spindle cell sarcoma (n = 2), and clear cell sarcoma (n = 1). Most patients had received prior systemic therapy (92.3%), and 9 (69.2%) had metastatic disease (Fig. 1c).

To establish a clinical comparison cohort, patients who were not included in the PDO-guided cohort (n = 14) and patients without established PDO models (n = 39) were considered for retrospective screening (Fig. 1d). Among 53 initially screened patients, 14 were excluded due to incomplete clinical information (n = 5) or unavailable follow-up data (n = 9). The remaining 39 eligible patients were included in the clinical comparison cohort (control cohort) for subsequent outcome analyses. Baseline balance between the PDO-guided and control cohorts was subsequently assessed using standardized mean differences (SMDs) for age, sex, histological subtype, previous lines of systemic therapy, and metastatic disease status, with all evaluated covariates showing absolute SMDs < 0.2 (Supplementary Fig. 1; Table 1).

Table 1

Baseline characteristics of patients in the PDO-guided and control cohorts. Demographic and clinical characteristics of patients included in the PDO-guided cohort (n = 13) and control cohort (n = 39). Continuous variables are presented as median (range), and categorical variables are presented as n (%). Standardized mean differences (SMDs) were used to evaluate baseline balance between cohorts. Characteristics related to PDO generation and follow-up are additionally summarized for patients receiving PDO-guided treatment.

Characteristic	Category	Control Cohort(N = 39)	PDO-Guided Cohort(N = 13)	SMD
Age, years	Median (range)	44 (9–74)	44 (13–70)	0.10
	< 15	2 (5)	1 (7.7)	
	15–40	19 (48.8)	4 (30.7)	
	≥ 40	18 (46.2)	8 (61.6)	
Sex	Male	24 (61.5)	9 (69.2)	0.16
	Female	15 (38.5)	4 (30.8)	
Histological subtype	UPS	16 (41.0)	5 (38.4)	0.07
	Synovial sarcoma	10 (25.6)	3 (23.1)	
	Epithelioid sarcoma	4 (10.3)	2 (15.4)	
	Spindle cell sarcoma	5 (12.8)	2 (15.4)	
	Clear cell sarcoma	4 (10.3)	1 (7.7)	
Previous lines of systemic therapy	0(treatment-naive)	9 (23.1)	1 (7.7)	0.18
	1	7 (17.9)	3 (23.1)	
	2	6 (15.4)	3 (23.1)	
	≥ 3	17 (43.6)	6 (46.2)	
Metastatic disease	Yes	27 (69.2)	9 (69.3)	0.00
	No	12 (30.8)	4 (30.7)	
PDO Generation & Follow-up				
Disease progression after sample collection	Yes	—	5 (38.5)	
	No	—	8 (61.5)	
Specimen source for PDO	Surgical resection	—	10 (76.9)	
	Biopsy	—	1 (7.7)	
	Other	—	2 (15.4)	
Tumor site used for PDO generation	Primary lesion	—	10 (76.9)	
	Metastatic lesion	—	2 (15.4)	
	Other	—	1 (7.7)	

To evaluate whether PDO-guided treatment translated into improved disease control, we compared cumulative progression-free survival between the two cohorts. Cumulative progression-free survival (PFS) duration was defined as the sum of progression-free intervals across sequential systemic treatment lines, starting from initiation of first-line treatment. Patients without sufficient follow-up information required for cumulative PFS calculation were excluded. Ultimately, 9 patients in the PDO-guided cohort and 28 patients in the control cohort were included in the analysis. Kaplan–Meier analysis demonstrated that patients in PDO-guided cohort exhibited longer cumulative PFS (log-rank P = 0.016; Fig. 1e).

The median cumulative PFS was 18.88 months and 6.22 respectively (Supplementary Table 2). These findings confirm that PDO-guided treatment confers a significant clinical benefit in achieving prolonged disease control in TUD patients.

a Kaplan-Meier analysis comparing first-line progression-free survival (PFS1) between the PDO-guided and control cohorts. Only patients receiving PDO-guided treatment as first-line therapy were included in the PDO-guided group. **b** Kaplan-Meier analysis of second-line progression-free survival (PFS2) in the control cohort. **c** Kaplan-Meier analysis of third-line progression-free survival (PFS3) in the control cohort. **d** Individual Effective PFS ratios in patients receiving PDO-guided treatment. The red dashed line indicates the clinical benefit threshold (PFS ratio ≥ 1.3). PFS_n: PDO-guided treatment, PFS_{n-1}: previous treatment line or DFS, *Patients whose Effective PFS ratios were calculated as PFS1/DFS. **e** Distribution of PFS1/DFS ratios in the PDO-guided and control cohorts. The red dashed line indicates the threshold of 1.3.

Treatment line-specific and intra-patient analyses of progression-free survival.

Given the longer cumulative PFS observed in the PDO-guided cohort, we further examined progression-free survival across individual treatment lines. Evaluable PFS1 data were available for 6 patients in the PDO-guided cohort and 28 in the control cohort, with median PFS1 of 2.00 and 1.77 months, respectively (log-rank P = 0.046; Fig. 2a). For PFS2, 4 PDO-guided patients and 22 controls were evaluable, with corresponding median values of 2.40 and 2.30 months, respectively (Fig. 2b). For PFS3, 3 patients in the PDO-guided cohort and 15 patients in the control cohort were evaluable, with median values of 2.56 and 0.92 months, respectively (Fig. 2c; Table 2). Given the small sample sizes, PFS2 and PFS3 were summarized descriptively without formal between-group comparisons.

Table 2
Disease-free survival and progression-free survival across treatment lines in the control cohort

Characteristics	DFS cohort		First-line PFS cohort		Second-line PFS cohort		Third-line PFS cohort	
	Patients, n (%)	mDFS (95% CI)	Patients, n (%)	mPFS (95% CI)	Patients, n (%)	mPFS (95% CI)	Patients, n (%)	mPFS (95% CI)
Total	36 (100.0)	6.4 (4.9–7.4)	28 (100.0)	1.7 (1.6-2.0)	22 (100.0)	2.3 (0.8–3.8)	15(100.0)	0.9 (0.8–1.1)
UPS	15 (41.7)	5.8 (2.4–9.2)	11 (39.4)	1.8 (0.4–3.2)	9 (40.9)	1.8 (1.8–1.9)	5 (33.3)	0.8 (0.4–1.2)
Synovial sarcoma	9 (25.0)	10.1 (5.0–15.0)	9 (32.1)	1.3 (1.2–1.4)	7 (31.8)	5.0 (0.8–9.2)	5 (33.3)	0.9 (0.6–1.2)
Epithelioid sarcoma	4 (11.1)	8.6 (2.9–14.3)	3 (10.7)	2.1 (0.4–3.8)	2 (9.1)	-	1 (6.7)	-
Spindle cell sarcoma	5 (13.9)	3.8 (2.1–5.6)	2 (7.1)	-	1 (4.6)	-	1 (6.7)	-
Clear cell sarcoma	3 (8.3)	2.3 (0.6-4.0)	3 (10.7)	1.1 (0.9–3.2)	3 (13.6)	1.5 (0.0–3.0)	3 (20.0)	0.7 (0.4-1.0)

Survival outcomes are presented as median survival time (months) with 95% confidence intervals (CIs). Median disease-free survival (mDFS) was calculated from definitive surgery to the date of disease recurrence or metastasis. Median progression-free survival (mPFS) was calculated from the initiation of each treatment line to radiological disease progression or death from any cause. Survival estimates were generated using the Kaplan–Meier method. A dash (-) indicates that the median survival time could not be estimated due to limited events or insufficient follow-up. UPS, undifferentiated pleomorphic sarcoma; DFS, disease-free survival; PFS, progression-free survival; CI, confidence interval.

At the individual-patient level, we calculated the Effective PFS ratio by comparing the PFS after PDO-guided treatment with the disease-control duration before PDO intervention. Among seven patients with evaluable paired data, Effective PFS ratios ranged from 0.12 to 7.32, with four patients achieving an Effective PFS ratio ≥ 1.3, the predefined threshold for clinical benefit[15] (Fig. 2d). Exploratory analysis of PFS1/DFS ratios showed that all patients in the PDO-guided cohort (n = 4) had ratios > 1.3, whereas ratios in the control cohort were generally below 1.3 (Fig. 2e).

Collectively, PFS1 differed significantly between the two cohorts, while the intra-patient analyses identified clinical benefit in a subset of patients receiving PDO-guided treatment.

a Representative bright-field images of PDOs established from tumor specimens with TUD. Scale bars, 200 μm (upper panels) and 100 μm (lower panels). **b** H&E staining and immunostaining for Ki-67 (marker of proliferation), CD99 (cluster of differentiation 99), EMA (epithelial membrane antigen) and SOX10 (SRY-box transcription factor 10) in parental tumor tissues and matched P3 PDOs. Scale bars, 60 μm. **c** Whole-exome sequencing (WES)-based comparison of somatic mutations between paired PTCs and P3 PDOs. Representative mutated genes and mutation types are shown. **d** Single nucleotide variant (SNV) spectra of paired PTCs and PDOs, showing the relative proportions of six nucleotide substitution types (C > A, C > G, C > T, T > A, T > C and T > G). **e** Distribution of variant classifications in paired PTCs and PDOs, including missense,

frameshift, in-frame, stop-gain and multi-hit alterations. **f** Genome-wide copy number variation (CNV) profiles of paired PTCs and PDOs across chromosomes 1–22, shown as log2(CNV) values. PTC, parental tumor cell; PDO, patient-derived organoid; P3, passage 3.

TUD-derived PDOs recapitulate key characteristics of parental tumors.

TUD-derived PDOs exhibited compact three-dimensional structures with heterogeneous growth patterns under bright-field microscopy (Fig. 3a). Hematoxylin and eosin (H&E) staining showed that PDOs recapitulated the morphological features of their parental tumors. Furthermore, immunohistochemical analysis of Ki67, CD99, EMA, and SOX10 revealed similar staining patterns between parental tumors and matched PDOs, indicating preservation of key tumor phenotypes during ex vivo propagation (Fig. 3b).

We further assessed genomic consistency between parental tumors and matched PDOs using whole-exome sequencing (WES). PDOs retained major genomic alterations detected in parental tumors, including representative alterations in TP53, SETD2, ATRX, and STAG2 (Fig. 3c). SNV spectra showed concordant substitution patterns between parental tumors and PDOs across the six major nucleotide substitution types (C > A, C > G, C > T, T > A, T > C, and T > G) (Fig. 3d). Variant classifications were also comparable, with missense mutations predominating in both groups (Fig. 3e). Genome-wide CNV profiling further showed similar patterns of copy number gains and losses across chromosomes 1–22 (Fig. 3f). Together, these findings demonstrate that TUD-derived PDOs recapitulate key histological, immunophenotypic, and genomic characteristics of their parental tumors.

a Distribution of drug sensitivity tests across therapeutic categories. **b** Tumor growth inhibition (TGI%) profiles of different therapeutic categories. **c** Ranking of therapeutic regimens by median TGI across PDO models. **d** Heatmap showing drug response profiles of individual PDO models and therapeutic regimens. Each row represents an individual PDO model.

PDO drug profiling identifies heterogeneous treatment responses and high activity of doxorubicin-based regimens in TUD.

To characterize treatment responses in TUD, PDO models established from 24 patients were subjected to drug sensitivity profiling. A total of 47 treatment regimens, including 22 single-agent and 25 combination regimens, were evaluated, of which 28 were tested in at least three independent PDO models. Chemotherapy represented the largest therapeutic category, followed by immunotherapy plus targeted therapy and immunotherapy (Fig. 4a). Doxorubicin-based combinations showed relatively high tumor growth inhibition (TGI) (Fig. 4b). We further ranked individual regimens according to their median TGI values. Doxorubicin plus pembrolizumab and doxorubicin plus atezolizumab showed the highest median TGI values (77.34% and 76.32%), numerically exceeding that of conventional doxorubicin plus ifosfamide (AI; 73.24%) (Fig. 4c). Consistently, anthracycline-based regimens showed broadly high TGI values across multiple PDO models (Fig. 4d). Drug responses nevertheless varied substantially among individual PDO models (Fig. 4b,d). Overall, doxorubicin-based regimens, particularly ICI-containing combinations, showed relatively high activity across the TUD-derived PDO screening.

a Clinical course and PDO-guided treatment of Case 1 (TUD-04). **b** Representative Calcein-AM/PI staining of PDOs following different treatments. **c** Quantification of TGI% across tested therapeutic regimens. **d** Serial CT images before and after GD-based treatment, with tumor lesions highlighted by red circles. **e** Clinical course and treatment of Case 2 (TUD-07). **f** Representative Calcein-AM/PI staining of PDOs following different treatments. **g** Quantification of TGI% across tested therapeutic regimens. **h** Serial MRI images before and after DOX + IFO+ DTIC treatment, with tumor lesions highlighted by red circles. **i** Clinical course and PDO-guided adjuvant treatment of Case 3 (TUD-01). **j** Representative Calcein-AM/PI staining of PDOs following different treatments. **k** Quantification of TGI% across tested therapeutic regimens. **l** MRI and X-ray imaging during follow-up, with tumor lesions highlighted by red circles. Scale bars, 500 μm (b, f, j).

Clinical outcomes following PDO-guided treatment in representative cases.

All 13 patients receiving PDO-guided treatment were followed clinically and included in outcome analyses. Three representative cases were selected, with PDOs established from metastatic lesions, recurrent tumors, and primary surgical specimens, respectively.

In Case 1 (TUD-04), a patient with metastatic UPS developed pulmonary and pleural metastases after surgury. Before PDO-guided treatment, the patient received several systemic regimens, including tislelizumab plus eribulin, eribulin monotherapy, and tislelizumab plus apatinib. Despite these treatments, CT imaging in January 2023 showed enlargement of multiple pulmonary and pleural metastatic lesions, indicating disease progression. PDOs were established from pleural effusion for drug response profiling (Fig. 5a). Calcein-AM/PI assessment identified gemcitabine plus docetaxel (GD) as the regimen with the highest TGI (51.30%) (Fig. 5b,c). PDO-guided GD-based therapy was initiated in February 2023, followed by marked regression of pleural metastases on serial CT imaging (Fig. 5d). Disease progression occurred in August 2023, corresponding to a PFS of 6 months.

In Case 2 (TUD-07), a patient with synovial sarcoma of the right foot underwent tumor resection in June 2022, followed by extended resection in July 2022. The patient developed an early local recurrence shortly after surgery and subsequently received AI, radiotherapy, and additional IFO treatment. In April 2025, the patient developed another local recurrence in the right plantar region, with imaging suggesting possible involvement of the adjacent bone. Recurrent tumor tissue obtained by biopsy in May 2025 was used for PDO establishment (Fig. 5e). Drug profiling identified

doxorubicin, ifosfamide, and dacarbazine (DOX + IFO+ DTIC) as the most active regimen, with a TGI of 99.77% (Fig. 5f,g).The patient subsequently received PDO-guided DOX + IFO +DTIC treatment and maintained local disease control on MRI, with a PFS of more than 13 months at the latest follow-up in July 2026 (Fig. 5h).

In Case 3 (TUD-01), a patient with UPS underwent PDO establishment from the primary surgical specimen to evaluate postoperative adjuvant treatment options (Fig. 5i). Doxorubicin plus dacarbazine and anti-PD-1 (DOX+ DTIC+ anti-PD-1) showed the highest TGI (58.89%), followed by AI (55.25%) (Fig. 5j,k). Notably, the patient had previously achieved radiological tumor shrinkage with neoadjuvant AI, consistent with the PDO sensitivity profile. Based on PDO profiling, DOX+ DTIC+ anti-PD-1 was selected as postoperative adjuvant therapy. Serial MRI and X-ray imaging showed sustained disease control (Fig. 5l), with a DFS of 24.6 months until recurrence in July 2025, compared with a median DFS of 5.8 months among patients with UPS in the control cohort (Table 2). Together, these representative cases showed concordance between PDO-derived drug sensitivity profiles and subsequent clinical treatment responses.

a Distribution of PDO sampling time points and concordance between PDO drug sensitivity profiles and clinical treatment responses. **b** Relationship between prior therapy lines and maximum PDO inhibition rate, assessed by Spearman correlation analysis and violin plots. **c** Kaplan–Meier analysis of time to new lesions according to the inhibition rate of the PDO-guided treatment regimen.

PDO drug sensitivity reflects treatment-related heterogeneity and informs subsequent treatment response.

PDO samples were obtained at different stages of the disease course, including before neoadjuvant therapy, at surgery and after recurrence or metastatic progression (Fig. 6a). Clinical responses were concordant with PDO sensitivity profiles in 12 of 13 patients receiving PDO-guided treatment (92.3%) (Fig. 6a). Concordance was defined as achieving partial response (PR) or stable disease (SD) at the first available radiological assessment after initiation of PDO-guided treatment.

We next investigated prior treatment exposure as a potential factor associated with inter-patient variability in PDO drug sensitivity. Across the 24 PDO models, the number of prior systemic therapy lines was negatively correlated with the maximum PDO TGI (Spearman r = − 0.46, P = 0.024). Median maximum PDO TGI was highest in treatment-naive patients (76.3%) and lower in those who had received 1, 2, or ≥ 3 prior lines (55.8%, 44.8%, and 49.4%, respectively; Fig. 6b; Supplementary Table 3). Finally, we examined the relationship between PDO drug sensitivity and subsequent disease control. TGI values for clinically administered PDO-guided regimens ranged from 28.52% to 99.77% (median, 61.33%). Using the median inhibition rate as the cutoff, patients were classified into a high inhibition group (> 61.33%) and a low inhibition group (≤ 61.33%). Time to new lesions was defined as the interval from PDO-guided therapy initiation to radiologically confirmed tumor recurrence or new metastasis, with event-free patients censored at the last follow-up. Kaplan–Meier analysis showed that patients in the high inhibition group had a significantly longer time to new lesions than those in the low inhibition group (log-rank P = 0.044; Fig. 6c).

Collectively, PDO drug sensitivity was concordant with clinical responses, with greater prior treatment exposure related to lower PDO sensitivity and higher PDO inhibitory activity linked to more sustained disease control.

Discussion

In this study, we evaluated a patient-derived organoid (PDO)-based drug sensitivity approach for treatment in tumors of uncertain differentiation (TUD), a rare group of soft tissue malignancies with limited therapeutic options[16,17]. By integrating PDO drug profiling with clinical treatment and follow-up, our study provides preliminary evidence for the feasibility of PDO-based functional testing in TUD.

Although some progress has been made in the treatment of TUD in recent years, the clinical benefits of new therapies remain relatively limited, and there are significant differences among patients. For example, t the XPO1 inhibitor selinexor achieved an ORR of only 2.7% in previously treated advanced dedifferentiated liposarcoma[18], while the ORR of the EZH2 inhibitor tazemetostat in advanced epithelioid sarcoma is approximately 15%[19]. While novel strategies such as MAGE-A4-targeted T-cell receptor therapy have demonstrated higher antitumor activity in synovial sarcoma, their application remains limited to patients who have undergone specific molecular screening[20]. In our study, among the 13 patients who received PDO-guided therapy, 12 (92.3%) had PDO drug sensitivity results that were consistent with their subsequent clinical treatment responses, supporting the potential of PDO as a patient-specific functional platform to aid in personalized treatment decisions. Furthermore, the PDO established in this study effectively preserves the histological characteristics of the parental tumor, providing a model foundation for the screening of patient-specific new drugs and combination therapy regimens, as well as a basis for the further development of functional companion diagnostics and standardized drug sensitivity testing strategies

Beyond treatment-response concordance, an important question is whether PDO-guided treatment translates into improved clinical outcomes. Previous studies have shown that in vitro PDO drug responses can reliably inform actual treatment responses in patients[21,22], while studies using sarcoma organoids have also observed consistency between in vitro drug responses and patient treatment outcomes[23]. Based on these findings, the cumulative PFS in the PDO-guided cohort in this study was significantly longer than that in the control cohort and a comparable difference was also observed in first-line PFS. Given the significant interpatient heterogeneity in TUD, we further adopted a patient-versus-self

design, in which 4 of the 7 evaluable patients had an effective PFS ratio ≥ 1.3. Therefore, the consistent results obtained from both the matched cohort and the patient-versus-self design further support the potential clinical value of PDO-guided therapy in TUD from two complementary perspectives; however, validation through larger-scale prospective studies is still required.

PDO drug sensitivity may be influenced by prior treatment exposure. In our study, overall PDO drug sensitivity decreased with increasing numbers of prior treatment lines. Repeated treatment may exert selective pressure on heterogeneous tumor cell populations, enriching drug-resistant or adaptive subclones and promoting the development of drug tolerance[24–26], which provides a possible biological explanation for the aforementioned phenomenon. More importantly, greater PDO sensitivity to the clinically administered regimen was linked to a longer interval before recurrence or new metastasis. Taken together, these results suggest that PDO drug sensitivity may reflect differences in tumor sensitivity related to prior treatment and provide clinically meaningful information for subsequent disease control.

The high in vitro activity of the doxorubicin–ICI combination observed in the PDO screening of this study aligns with the expanding clinical application of immunotherapy in high-grade soft tissue sarcomas in recent years. In the SU2C-SARC032 randomized trial, perioperative pembrolizumab improved disease-free survival (DFS) in patients with stage III limb soft tissue sarcoma, with the 2-year DFS rate increasing from 52% in the control group to 67% (HR = 0.61)[27]. In our study, among the 4 evaluable patients receiving ICI combination therapy, 3 demonstrated PDO responses consistent with actual clinical efficacy, providing preliminary evidence for further exploration of such combination regimens. Notably, in one patient with grade 3 UPS, the PDO recapitulated sensitivity to prior neoadjuvant AI therapy while showing greater sensitivity to DOX + DTIC + ICI, followed by a DFS of 24.6 months after PDO-informed adjuvant treatment. Although PDOs cannot fully recapitulate tumor–immune interactions in vivo, these findings support further investigation of PDO-based testing for ICI-containing regimens in TUD.

Several limitations should be considered when interpreting these findings. Due to the rarity of TUD, the PDO-guided treatment cohort was relatively small, limiting the statistical power of subgroup analyses. The retrospective and non-randomized design, together with heterogeneous treatment patterns, may have introduced selection bias and residual confounding despite cohort matching. In addition, PDO models primarily reflect tumor cell-intrinsic drug responses and do not fully reproduce immune interactions, pharmacokinetic factors, or tumor microenvironmental effects[28,29].

In summary, our findings support PDO-based drug sensitivity testing as a functional complement to individualized treatment in TUD. By providing patient-specific treatment-response information beyond conventional pathological and molecular assessments, PDO profiling may help inform therapeutic decision-making in rare and heterogeneous malignancies. Prospective validation is needed to establish its clinical utility.

Methods

Study design and clinical cohort

Tumor specimens and clinical information used in this study were obtained from Shanghai Sixth People's Hospital. Written informed consent was obtained from all patients for the use of tumor tissues and clinical data for research purposes. This study was approved by the Institutional Review Board of Shanghai Sixth People's Hospital (approval number: 2024-KY-204(K)) and was conducted in accordance with the Declaration of Helsinki.

This single-center retrospective cohort study included patients with TUD treated between February 2020 and July 2026. TUD was diagnosed according to the World Health Organization (WHO) classification of soft tissue tumors and included undifferentiated pleomorphic sarcoma (UPS), synovial sarcoma, epithelioid sarcoma, spindle cell sarcoma, clear cell sarcoma, and alveolar soft part sarcoma. Patients included in the PDO-guided cohort met the following criteria: (i) histologically confirmed TUD; (ii) availability of tumor specimens for PDO establishment; (iii) successful PDO generation with completed drug sensitivity testing; and (iv) availability of complete treatment records and clinical follow-up data. Patients were classified into the PDO-guided cohort when PDO drug sensitivity results were incorporated into subsequent treatment selection.

To evaluate clinical outcomes associated with PDO-guided treatment selection, a control cohort was established by screening patients treated during the same study period who were not included in the PDO-guided cohort or did not have established PDO models. Demographic and clinical data, including age, sex, histological subtype, disease status, prior treatment history, number of previous lines of systemic therapy, and subsequent therapeutic regimens, were retrospectively collected from electronic medical records. Patients with incomplete clinical information or unavailable follow-up data were excluded. Baseline balance between the PDO-guided and control cohorts was assessed using standardized mean differences (SMDs) for age, sex, histological subtype, metastatic disease status, and number of previous lines of systemic therapy, with an absolute SMD < 0.2 considered indicative of adequate balance[30]. Clinical outcomes were assessed according to treatment setting. Disease-free survival (DFS) was defined as the time from curative-intent surgery to disease recurrence or metastasis. Progression-free survival (PFS) was defined as the time from initiation of systemic therapy for recurrent or metastatic disease to radiologically confirmed disease progression. PFS1, PFS2, and PFS3 represented PFS during first-, second-, and third-line systemic therapy, respectively.

Patient sample collection and processing

Tumor tissues were immediately transferred into sterile containers containing pre-cooled tissue preservation solution after surgical excision or biopsy and transported to the laboratory at 2–8°C. All specimens were processed within 24 h after collection for PDO establishment. Upon arrival, tumor tissues were examined, and necrotic, adipose, and calcified components were removed. Samples were washed with Dulbecco's phosphate-buffered saline (DPBS) containing antibiotics and mechanically minced into small fragments (approximately 1–2 mm^3). Tissue fragments were enzymatically dissociated using collagenase IV (1 mg/mL) and hyaluronidase (20 μg/mL) at 37°C for 15–60 min until single cells or small cell clusters were obtained. Digestion was terminated using DPBS supplemented with antibiotics and fetal bovine serum (FBS), followed by filtration through a 100 μm cell strainer and centrifugation to collect cell pellets. For malignant effusion-derived samples, collected fluids were centrifuged to enrich cellular components, followed by filtration, and repeated washing. Red blood cells were removed using RBC lysis buffer when necessary. Cell number and viability were assessed using acridine orange/propidium iodide (AO/PI) staining. Viable cell suspensions were subsequently used for PDO establishment. Detailed information regarding PDO culture supplements is provided in Supplementary Table 4.

Establishment and maintenance of patient-derived organoids

Following tissue dissociation, viable cells were counted and embedded in Matrigel Matrix GFR Phenol Red Free (Modigen, Cat. No. 082703T) for PDO establishment. Cell–matrix suspensions were seeded into 96 culture plates and allowed to polymerize, followed by addition 100 μL of organoid complete medium (OneTar-PDO-T100, OneTar, Shanghai, China). PDOs were maintained at 37°C with 5% CO_2, and culture medium was replaced every 2–3 days. Organoid formation, growth, and morphology were monitored by inverted microscopy throughout the culture period. Established PDOs were expanded by serial passaging under the same culture conditions and subsequently used for downstream drug sensitivity assays. For long-term storage, expanded PDOs were cryopreserved in organoid freezing medium and stored in liquid nitrogen for subsequent recovery and analysis.

Histological and immunohistochemical assessment

To assess the morphological and phenotypic fidelity of PDOs relative to matched parental tumors, PDOs and corresponding tumor specimens were formalin-fixed, paraffin-embedded, and analyzed by hematoxylin and eosin (H&E) staining and immunohistochemistry (IHC). H&E staining was performed to evaluate the preservation of tumor architecture and cellular morphology. For immunophenotypic characterization, paraffin-embedded sections were subjected to deparaffinization, rehydration, antigen retrieval, and blocking according to standard immunohistochemical procedures. Sections were incubated with antibodies against Ki-67, CD99, EMA, and SOX10 to assess the retention of key proliferative and lineage-associated features of parental tumors. Ki-67 was used to evaluate proliferative activity, whereas CD99, EMA, and SOX10 were selected based on their established relevance in the characterization and differential diagnosis of soft tissue sarcomas, including tumors of uncertain differentiation. Representative images were acquired using an automated digital slide scanning system for comparative evaluation of PDOs and matched parental tumors.

Whole exome sequencing and mutational profiling

Genomic DNA was extracted from matched parental tumor tissues and corresponding PDOs. The concentration and quality of extracted DNA were assessed before library preparation, and samples meeting the predefined quality requirements were subjected to whole-exome sequencing (WES). Whole-exome libraries were prepared using an exome capture-based approach and sequenced on an Illumina NovaSeq 6000 platform using paired-end 150-bp reads. Raw sequencing reads were subjected to quality control to remove adapter-contaminated and low-quality reads. High-quality reads were aligned to the human reference genome (GRCh38) using the Burrows–Wheeler Aligner (BWA). The resulting alignment files were subsequently processed according to the Genome Analysis Toolkit (GATK) best-practice workflow. Single-nucleotide variants (SNVs) and small insertions and deletions (indels) were identified using GATK Mutect2 and subjected to quality filtering to obtain high-confidence variant calls. Variants were subsequently annotated using ANNOVAR. Common germline polymorphisms were excluded based on population allele frequencies in public population databases. To assess the preservation of genomic characteristics in PDOs relative to their matched parental tumors, high-confidence variants identified in paired samples were compared at the gene and variant levels. Shared and sample-specific alterations were identified, and the distribution of variant classes and single-nucleotide substitution patterns was further characterized. These analyses were used to evaluate the extent to which PDOs retained the major mutational features of their corresponding parental tumors.

PDO-based drug sensitivity testing

For drug sensitivity profiling, established PDOs were dissociated into single-cell suspensions and embedded in Matrigel-coated 96-well plates according to the predefined screening design. Following organoid formation, PDO cultures were evaluated for suitability for drug sensitivity testing based on organoid formation, baseline viability, and the presence of sufficient evaluable organoid structures for quantitative analysis.

PDO cultures meeting these criteria were subsequently exposed to different therapeutic agents or vehicle controls for 4 days. Drug concentrations were selected based on clinically achievable plasma exposure levels, referring to reported maximum plasma concentrations (Cmax). Detailed information regarding tested drugs, concentrations, and vendors is provided in Supplementary Table 5.

Following treatment, PDO viability was assessed by Calcein AM/propidium iodide (PI) double fluorescence staining. Green fluorescence indicated viable cells, whereas red fluorescence represented dead cells. Fluorescence images were acquired using an inverted fluorescence microscope, and viability-associated signals were quantified by image analysis. The tumor growth inhibition (TGI) score was calculated based on the normalized green fluorescence intensity relative to vehicle-treated controls using the following formula:

$$TGI\ (\%) = [1 - (DG/R/CG/R)] \times 100\%$$

where DG/R represents the normalized green fluorescence integrated optical density (IOD) of drug-treated PDOs, and CG/R represents the corresponding value in vehicle-treated controls.

PDO-guided treatment and clinical outcome assessment

Treatment regimens were selected through routine clinical evaluation, incorporating PDO drug sensitivity results together with pathological diagnosis, previous treatment history, disease status, multidisciplinary team (MDT) discussion, and individual patient characteristics. PDO clinical concordance was assessed by comparing PDO-based drug sensitivity profiles with subsequent clinical responses following initiation of PDO-informed treatment. A concordant case was defined as a patient receiving a PDO-informed treatment regimen who achieved partial response (PR) or stable disease (SD) at the first radiological assessment after treatment initiation. For patients receiving PDO-guided treatment, PFS was calculated from the initiation of the PDO-informed treatment regimen to radiologically confirmed disease progression. Patients without documented disease progression were censored at the date of the last follow-up. To evaluate the association between PDO drug sensitivity and clinical outcomes, patients were stratified according to the inhibitory activity of the corresponding clinical regimen in PDO assays. The corresponding regimen was defined as the treatment regimen actually administered after PDO-guided decision-making. Patients were categorized into higher and lower PDO inhibitory activity groups according to the median inhibitory activity value. For the Kaplan-Meier analysis comparing time to new lesions between the higher and lower PDO inhibitory activity groups (Fig. 6c), a specific endpoint definition was applied, with time to new lesions development was defined as the interval from PDO-guided therapy initiation to radiologically confirmed tumor recurrence or new metastasis, with event-free patients censored at the last follow-up

An intra-patient comparison analysis was performed using the Effective PFS ratio. The Effective PFS ratio was defined as the ratio of PFS duration during PDO-guided treatment to the disease-control duration achieved during the immediately preceding treatment period before PDO intervention. For patients receiving PDO-guided treatment after postoperative recurrence, the reference period was defined as DFS following initial treatment. For patients who had previously received systemic therapy for recurrent or metastatic disease before PDO intervention, the reference period was defined as the PFS achieved during the immediately preceding treatment line. An Effective PFS ratio ≥ 1.3 was considered indicative of relative clinical benefit according to previously established criteria. To further evaluate the relative change in disease control compared with prior disease status, PFS1/DFS ratio analysis was performed in patients with available first-line treatment and postoperative DFS information. As an exploratory analysis, the PFS1/DFS ratio was calculated as the duration of first-line PFS divided by the postoperative DFS duration.

Statistical analysis

Continuous variables were summarized as medians with interquartile ranges (IQRs), and categorical variables were presented as frequencies and percentages. The inhibitory activity profiles of therapeutic regimens evaluated in PDO assays were summarized descriptively. Baseline balance between the PDO-guided and control cohorts was assessed using standardized mean differences (SMDs). Survival outcomes were analyzed using the Kaplan-Meier method, and differences between survival distributions were assessed using the log-rank test. PFS analyses were performed according to predefined clinical settings, including PDO-guided treatment-associated outcomes and comparisons between the PDO-guided and control cohorts. Treatment-line-specific analyses included PFS1, PFS2, and PFS3. Formal between-group survival comparison was performed for PFS1, whereas PFS2 and PFS3 were summarized descriptively because of the limited number of patients receiving PDO-guided treatment. Patients were stratified according to the median inhibitory activity of the corresponding clinical regimen in PDO assays for survival analysis. The Effective PFS ratio was evaluated using intra-patient comparisons to assess relative changes in disease control before and after PDO-guided treatment. Correlations between previous treatment lines and maximum PDO inhibitory activity were assessed using Spearman correlation analysis. All statistical tests were two-sided, and P values < 0.05 were considered statistically significant. Statistical analyses were performed using GraphPad Prism 9.1.0 (GraphPad Software, San Diego, CA, USA) and R software version 4.3.2.

Declarations

Acknowledgements

This work was supported by the Medical New Technology Research and Transformation Seed Program of Shanghai Municipal Health Commission (Grant No. 2024ZZ2032) and the 2026 Medical New Technology Research and Transformation Growth Program (Class A) of Shanghai, China (Grant No. 2026CZA0102) and the National Natural Science Foundation of China (Grant No. 82673691). We acknowledge the support from Shanghai Sixth People's Hospital and appreciate the contributions of the clinical team involved in patient enrollment, sample collection, and clinical follow-up. We sincerely thank all patients and their families for their participation and contribution to this study. The funders had no role in the study design, data collection, analysis and interpretation of the data, or preparation of the manuscript.

Author contributions

Q. K., L.T. and C.Z. conceived and designed the study. Q.K. and C.Z. established patient-derived organoid models and performed drug sensitivity assays. L.T. contributed to pathological evaluation and clinical sample collection. Q.K. and C.Y. performed data analysis and statistical analysis. H.L., Y.W., Y.W. and Y.H. collected clinical data and performed patient follow-up. D.C. and Q.Y, contributed to clinical consultation and sample acquisition. Q.K. drafted the manuscript. A.H. and X.D supervised the study, interpreted the data and critically revised the manuscript. All authors reviewed and approved the final manuscript.

Competing interests

The authors declare that they have no competing interests.

References

1. Sbaraglia, M., Bellan, E. & Dei Tos, A. P. The 2020 WHO Classification of Soft Tissue Tumours: news and perspectives. *Pathologica* 113, 70–84 (2021).
2. Martínez-Trufero, J. *et al.* Uncommon and peculiar soft tissue sarcomas: Multidisciplinary review and practical recommendations for diagnosis and treatment. Spanish group for Sarcoma research (GEIS – GROUP). Part I. *Cancer Treatment Reviews* 99, (2021).
3. Gounder, M. M. *et al.* Clinical genomic profiling in the management of patients with soft tissue and bone sarcoma. *Nat Commun* 13, 3406 (2022).
4. Gamboa, A. C., Gronchi, A. & Cardona, K. Soft-tissue sarcoma in adults: An update on the current state of histiotype-specific management in an era of personalized medicine. *CA Cancer J Clin* 70, 200–229 (2020).
5. Gronchi, A. *et al.* Soft tissue and visceral sarcomas: ESMO–EURACAN–GENTURIS Clinical Practice Guidelines for diagnosis, treatment and follow-up. *Annals of Oncology* 32, 1348–1365 (2021).
6. Letai, A. Functional precision cancer medicine-moving beyond pure genomics. *Nat Med* 23, 1028–1035 (2017).
7. Sicklick, J. K. *et al.* Molecular profiling of cancer patients enables personalized combination therapy: the I-PREDICT study. *Nat Med* 25, 744–750 (2019).
8. Cobain, E. F. *et al.* Assessment of Clinical Benefit of Integrative Genomic Profiling in Advanced Solid Tumors. *JAMA Oncol* 7, 525–533 (2021).
9. Qu, S. *et al.* Patient-derived organoids in human cancer: a platform for fundamental research and precision medicine. *Mol Biomed* 5, 6 (2024).
10. Xiao, H. *et al.* Proteomics and Organoid Culture Reveal the Underlying Pathogenesis of Hashimoto's Thyroiditis. *Front Immunol* 12, 784975 (2021).
11. Jensen, L. H. *et al.* Precision medicine applied to metastatic colorectal cancer using tumor-derived organoids and in-vitro sensitivity testing: a phase 2, single-center, open-label, and non-comparative study. *J Exp Clin Cancer Res* 42, 115 (2023).
12. Wensink, G. E. *et al.* Patient-derived organoids as a predictive biomarker for treatment response in cancer patients. *NPJ Precis Oncol* 5, 30 (2021).
13. Xiao, Y. *et al.* Stereotactic body radiotherapy plus cadonilimab (PD-1/CTLA-4 bispecific antibody) as third-line or beyond therapy for refractory solid tumors: A phase 1b study. *Cancer Commun (Lond)* 45, 1235–1246 (2025).
14. Li, T. *et al.* First-Line Anlotinib Treatment for Soft-Tissue Sarcoma in Chemotherapy-Ineligible Patients: An Open-Label, Single-Arm, Phase 2 Clinical Trial. *Clin Cancer Res* 30, 4310–4317 (2024).
15. Von Hoff, D. D. *et al.* Pilot study using molecular profiling of patients' tumors to find potential targets and select treatments for their refractory cancers. *J Clin Oncol* 28, 4877–4883 (2010).
16. Choi, J. H. & Ro, J. Y. The 2020 WHO Classification of Tumors of Soft Tissue: Selected Changes and New Entities. *Adv Anat Pathol* 28, 44–58 (2021).
17. Von Mehren, M. *et al.* Soft Tissue Sarcoma, Version 2.2022. *J Natl Compr Canc Netw* 20, 815–833 (2022).

18. Gounder, M. M. *et al.* Selinexor in Advanced, Metastatic Dedifferentiated Liposarcoma: A Multinational, Randomized, Double-Blind, Placebo-Controlled Trial. *J Clin Oncol* 40, 2479–2490 (2022).
19. Krishnakumar, M., Zafar, M. & Reddy, A. Systemic therapy for advanced epithelioid sarcoma: A meta-analysis of effectiveness and safety study. *J Clin Oncol* 43, e23558–e23558 (2025).
20. D'Angelo, S. P. *et al.* SPEARHEAD-1: a single-arm phase 2 trial of afamitresgene autoleucel (afami-cel) in advanced synovial sarcoma and myxoid/round cell liposarcoma. *Lancet* 403, 1460–1471 (2024).
21. Boilève, A. *et al.* Organoids for Functional Precision Medicine in Advanced Pancreatic Cancer. *Gastroenterology* 167, 961–976.e13 (2024).
22. Cartry, J. *et al.* Implementing patient derived organoids in functional precision medicine for patients with advanced colorectal cancer. *J Exp Clin Cancer Res* 42, 281 (2023).
23. Al Shihabi, A. *et al.* The landscape of drug sensitivity and resistance in sarcoma. *Cell Stem Cell* 31, 1524–1542.e4 (2024).
24. Dagogo-Jack, I. & Shaw, A. T. Tumour heterogeneity and resistance to cancer therapies. *Nat Rev Clin Oncol* 15, 81–94 (2018).
25. Ramirez, M. *et al.* Diverse drug-resistance mechanisms can emerge from drug-tolerant cancer persister cells. *Nat Commun* 7, 10690 (2016).
26. Boumahdi, S. & de Sauvage, F. J. The great escape: tumour cell plasticity in resistance to targeted therapy. *Nat Rev Drug Discov* 19, 39–56 (2020).
27. Mowery, Y. M. *et al.* Pembrolizumab, radiation therapy, and surgery versus radiation therapy and surgery for stage III soft tissue sarcoma of the extremity: a randomised, open-label clinical trial. *Lancet* 404, 2053–2064 (2024).
28. Bose, S., Clevers, H. & Shen, X. Promises and Challenges of Organoid-Guided Precision Medicine. *Med* 2, 1011–1026 (2021).
29. Pauli, C. *et al.* Personalized In Vitro and In Vivo Cancer Models to Guide Precision Medicine. *Cancer Discov* 7, 462–477 (2017).
30. Austin, P. C. Balance diagnostics for comparing the distribution of baseline covariates between treatment groups in propensity-score matched samples. *Stat Med* 28, 3083–3107 (2009).

Figures

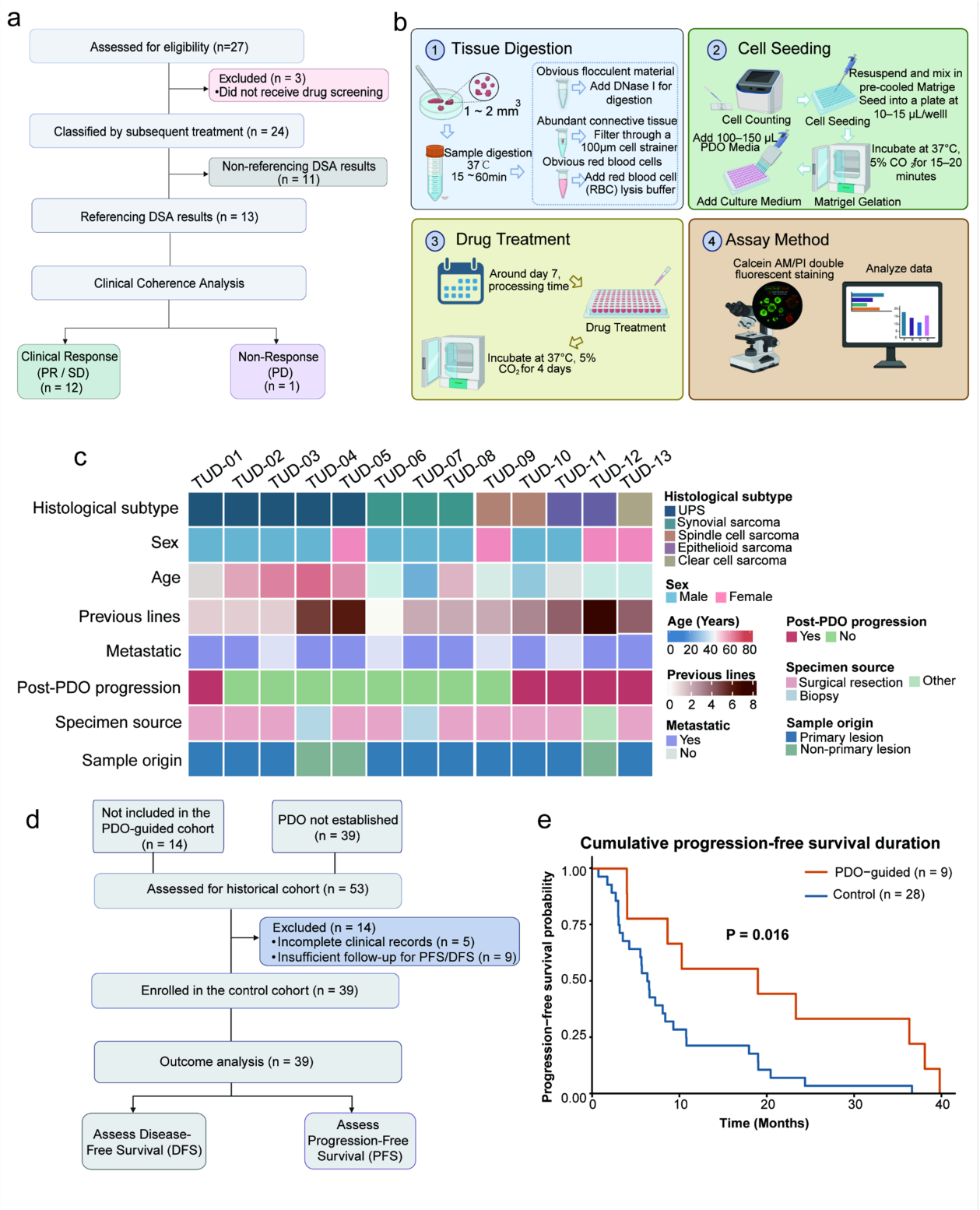


Figure 1

Establishment of PDO-guided cohorts and clinical outcome analysis in tumors of uncertain differentiation.

aEstablishment of the PDO-guided cohort. **b** Schematic workflow of PDO establishment and drug sensitivity assessment. **c** Baseline characteristics of patients included in the PDO-guided cohort. The heatmap summarizes clinicopathological features. **d** Establishment of the control cohort. **e** Kaplan-Meier analysis of cumulative progression-free survival (PFS) duration between the PDO-guided and control cohorts. The analysis included patients with evaluable progression-free survival intervals. DSA, drug sensitivity analysis.

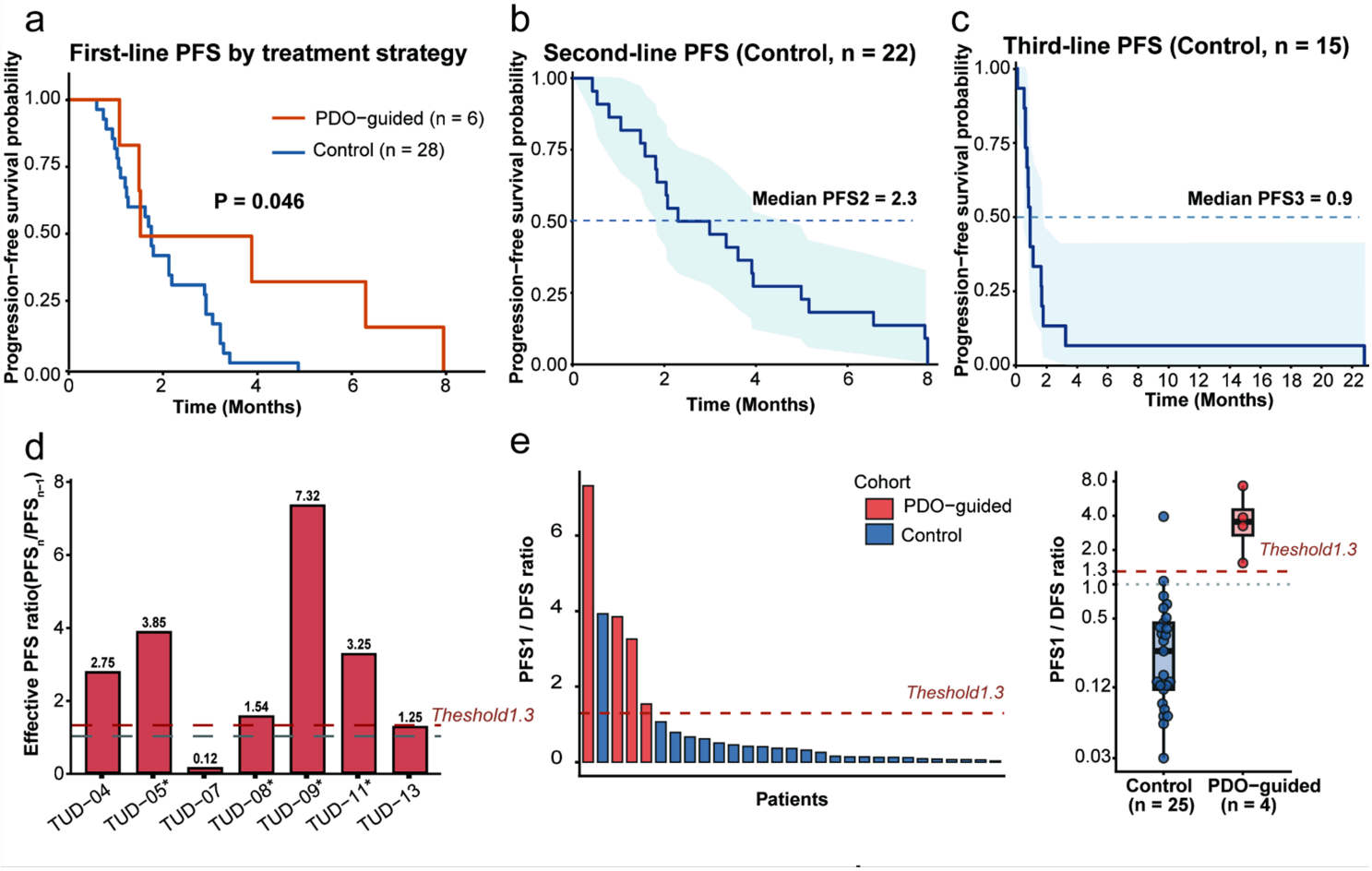


Figure 2

Establishment of PDO-guided cohorts and clinical outcome analysis in tumors of uncertain differentiation.

aEstablishment of the PDO-guided cohort. **b** Schematic workflow of PDO establishment and drug sensitivity assessment. **c** Baseline characteristics of patients included in the PDO-guided cohort. The heatmap summarizes clinicopathological features. **d** Establishment of the control cohort. **e** Kaplan-Meier analysis of cumulative progression-free survival (PFS) duration between the PDO-guided and control cohorts. The analysis included patients with evaluable progression-free survival intervals. DSA, drug sensitivity analysis.

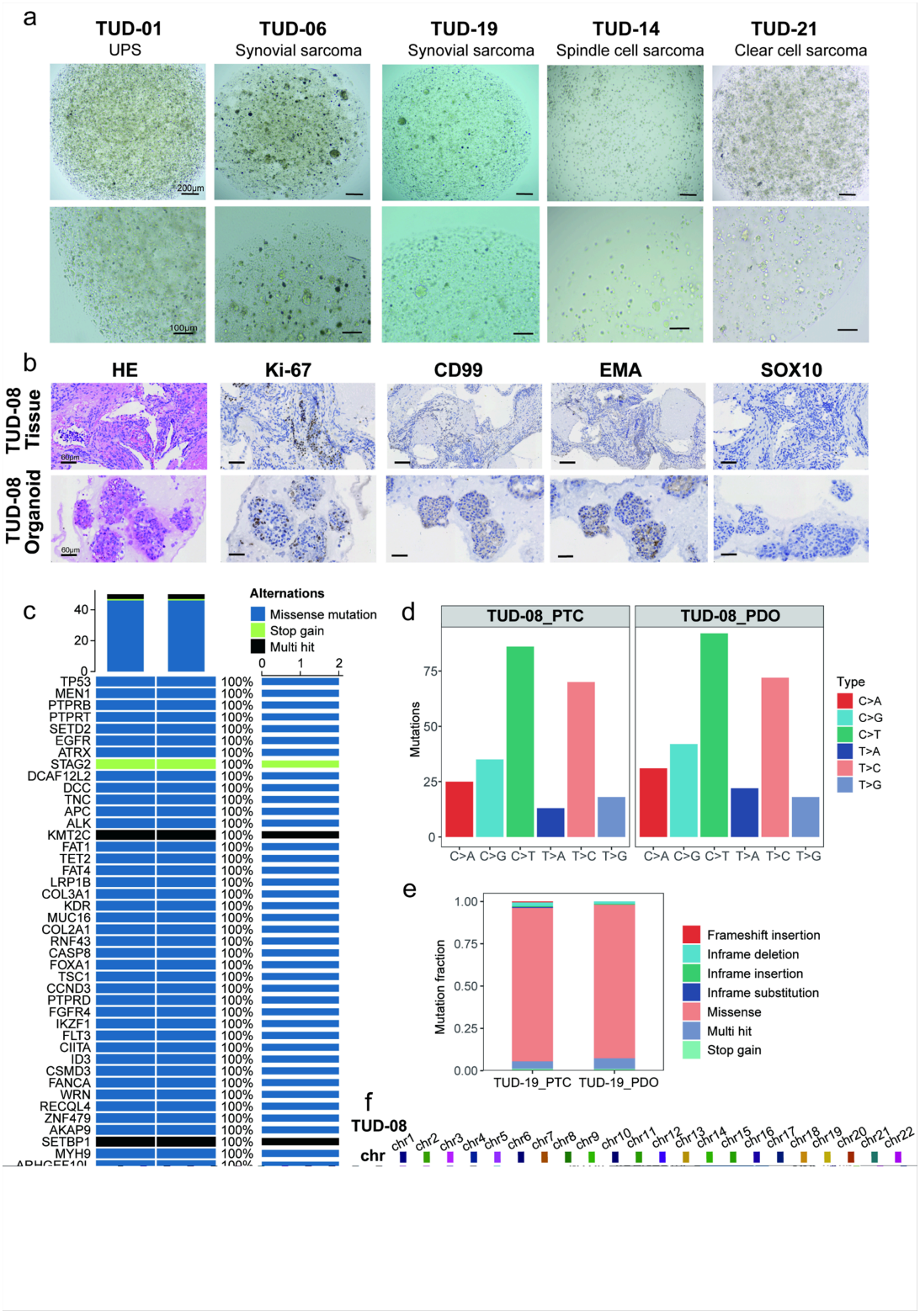


Figure 3

Patient-derived organoids retain histological and genomic features of tumors of uncertain differentiation.

a Representative bright-field images of PDOs established from tumor specimens with TUD. Scale bars, 200 μm (upper panels) and 100 μm (lower panels). **b** H&E staining and immunostaining for Ki-67 (marker of proliferation), CD99 (cluster of differentiation 99), EMA (epithelial membrane antigen) and SOX10 (SRY-box transcription factor 10) in parental tumor tissues and matched P3 PDOs. Scale bars, 60 μm. **c** Whole-exome sequencing (WES)-based comparison of somatic mutations between paired PTCs and P3 PDOs. Representative mutated genes and mutation types are shown. **d** Single nucleotide variant (SNV) spectra of paired PTCs and PDOs, showing the relative proportions of six nucleotide substitution types (C>A, C>G, C>T, T>A, T>C and T>G). **e** Distribution of variant classifications in paired PTCs and PDOs, including missense,

frameshift, in-frame, stop-gain and multi-hit alterations. **f** Genome-wide copy number variation (CNV) profiles of paired PTCs and PDOs across chromosomes 1–22, shown as log2(CNV) values. PTC, parental tumor cell; PDO, patient-derived organoid; P3, passage 3.

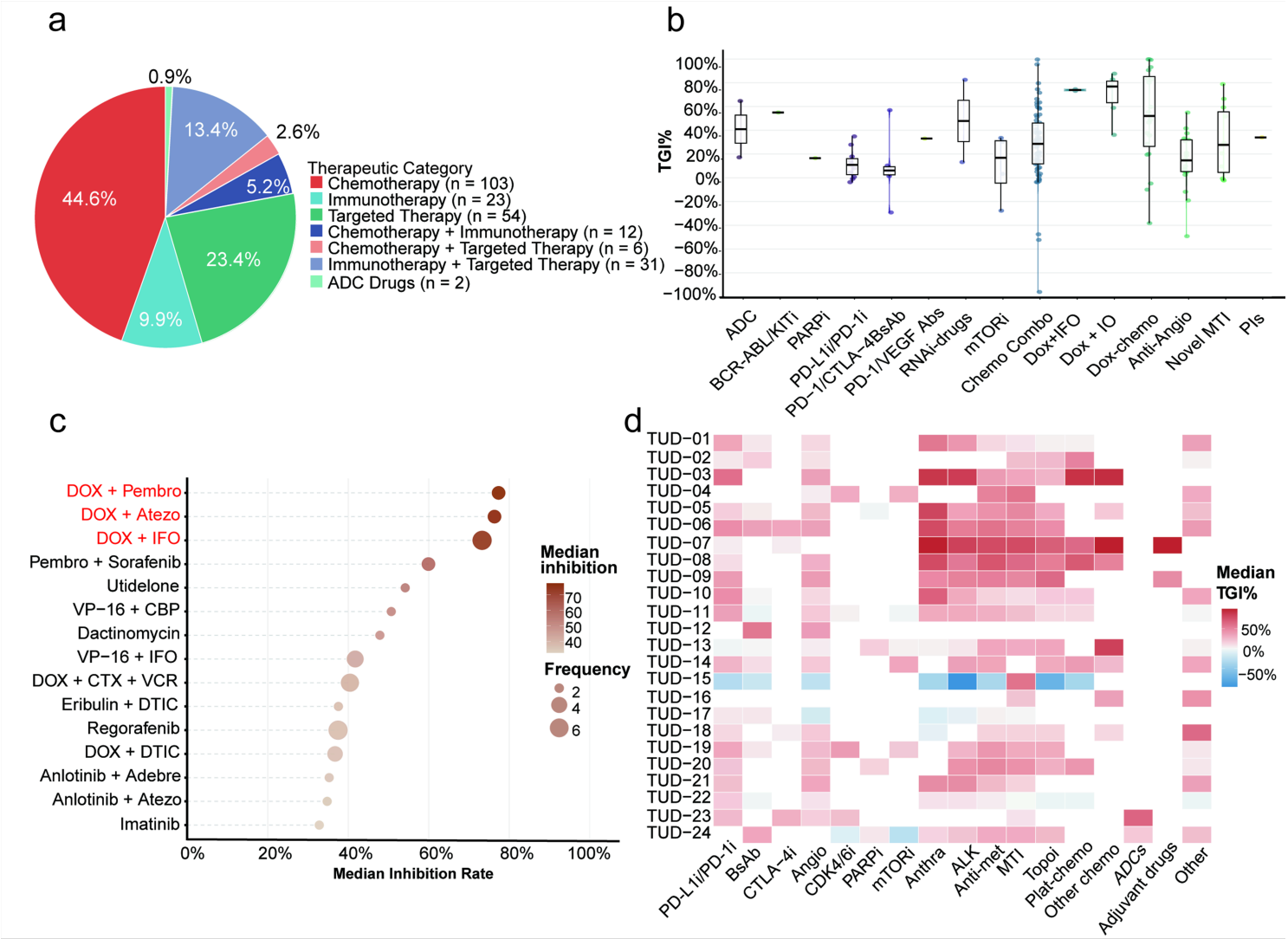


Figure 4

Drug sensitivity landscape of TUD-derived PDOs across diverse treatment regimens.

a Distribution of drug sensitivity tests across therapeutic categories. **b** Tumor growth inhibition (TGI%) profiles of different therapeutic categories. **c** Ranking of therapeutic regimens by median TGI across PDO models. **d** Heatmap showing drug response profiles of individual PDO models and therapeutic regimens. Each row represents an individual PDO model.

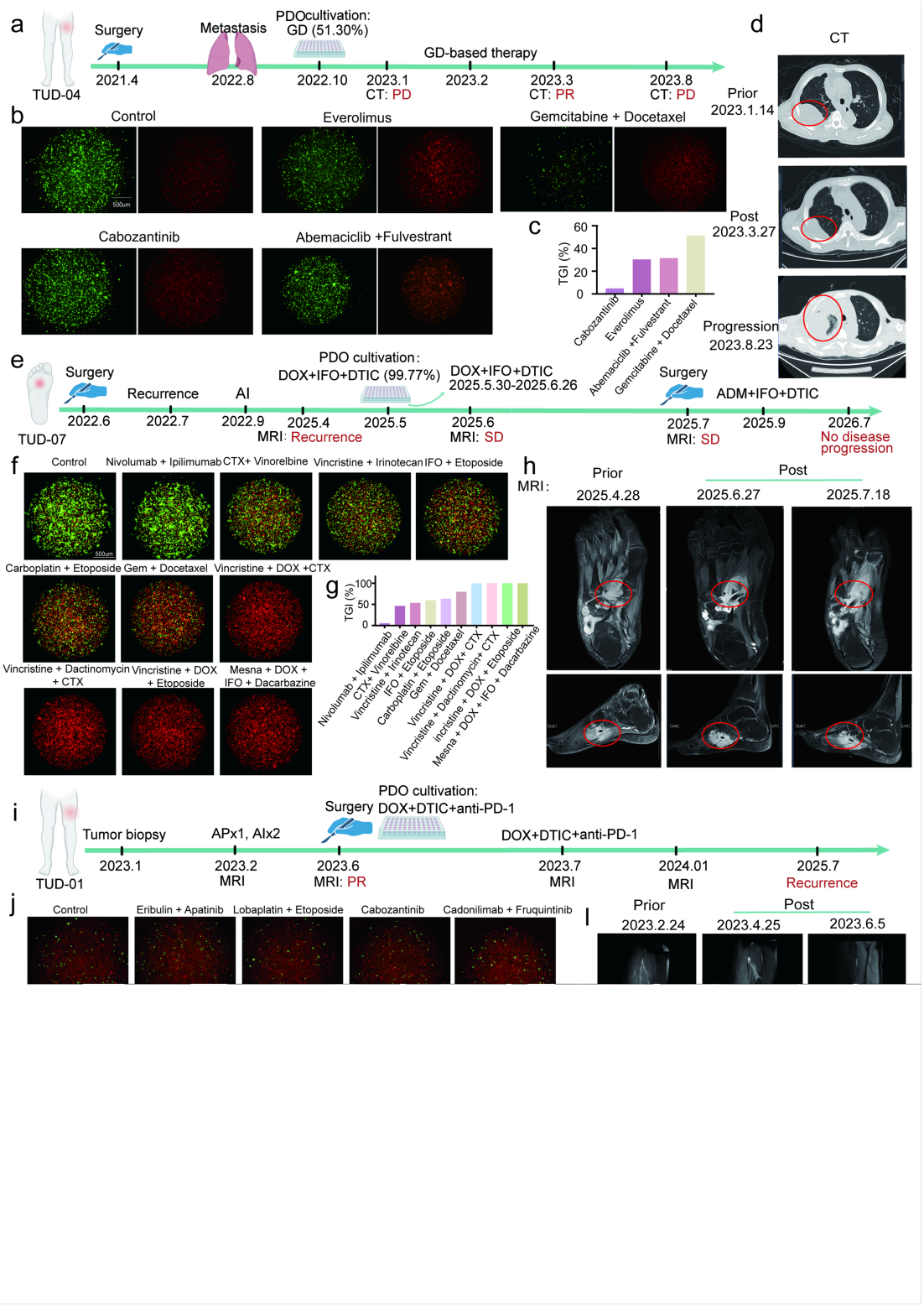


Figure 5

Clinical application of PDO-guided treatment in tumors of uncertain differentiation.

a Clinical course and PDO-guided treatment of Case 1 (TUD-04). **b** Representative Calcein-AM/PI staining of PDOs following different treatments. **c** Quantification of TGI% across tested therapeutic regimens. **d** Serial CT images before and after GD-based treatment, with tumor lesions highlighted by red circles. **e** Clinical course and treatment of Case 2 (TUD-07). **f** Representative Calcein-AM/PI staining of PDOs following different treatments. **g** Quantification of TGI% across tested therapeutic regimens. **h** Serial MRI images before and after DOX+ IFO+ DTIC treatment, with tumor lesions highlighted by red circles. **i** Clinical course and PDO-guided adjuvant treatment of Case 3 (TUD-01). **j**

Representative Calcein-AM/PI staining of PDOs following different treatments. **k** Quantification of TGI% across tested therapeutic regimens. **l** MRI and X-ray imaging during follow-up, with tumor lesions highlighted by red circles. Scale bars, 500 μm (b, f, j).

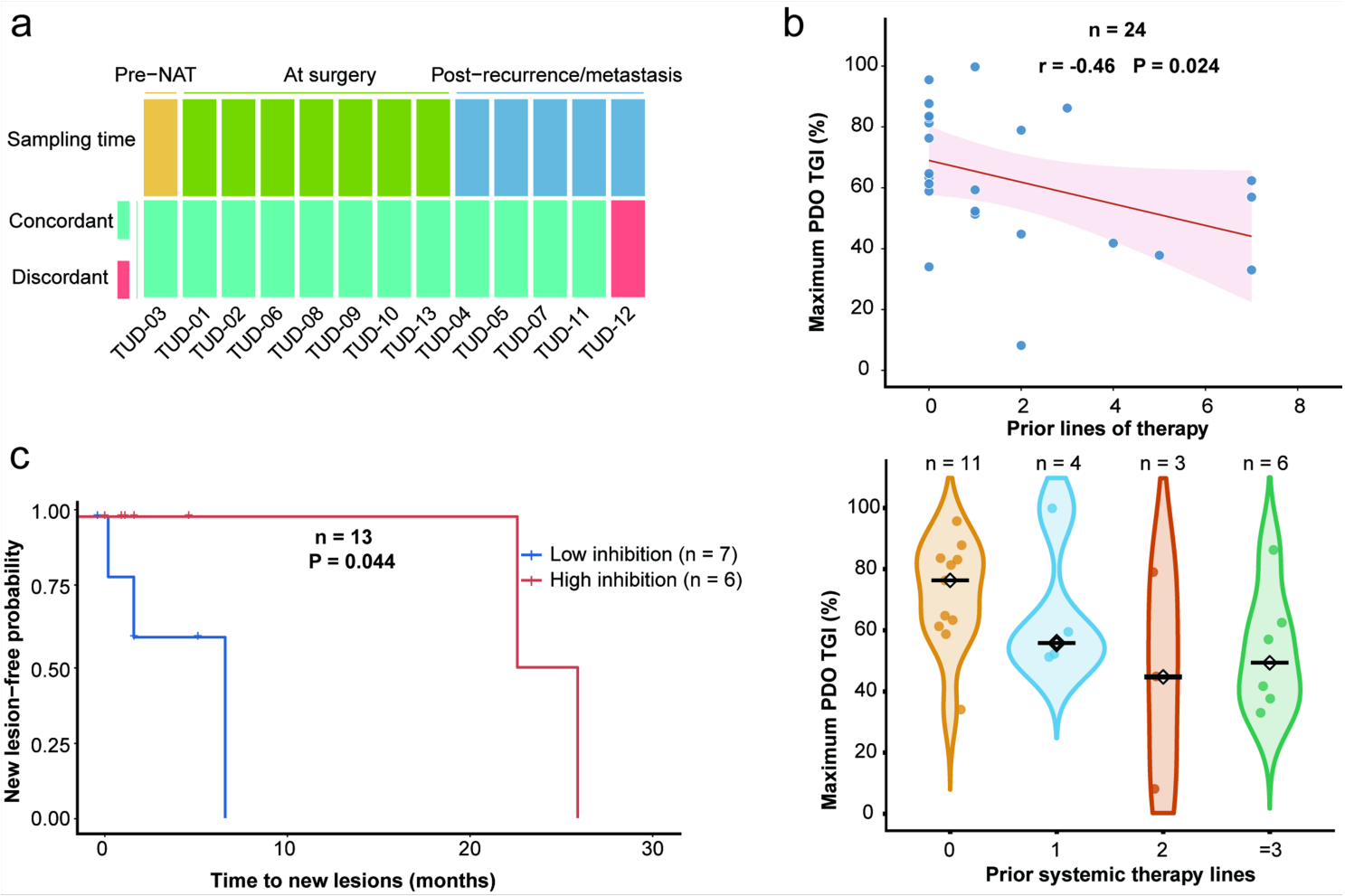


Figure 6

Treatment exposure and clinical implications of drug sensitivity variation in TUD-derived PDOs.

aDistribution of PDO sampling time points and concordance between PDO drug sensitivity profiles and clinical treatment responses. **b** Relationship between prior therapy lines and maximum PDO inhibition rate, assessed by Spearman correlation analysis and violin plots. **c** Kaplan–Meier analysis of time to new lesions according to the inhibition rate of the PDO-guided treatment regimen.

Supplementary Files

This is a list of supplementary files associated with this preprint. Click to download.

- table.docx
- SupplementaryInformation.pdf